15th Australasian Fluid Mechanics Conference
The University of Sydney, Sydney, Australia
13-17 December 2004

DETONATION MODELLING OF CORNER-TURNING SHOCKS IN PBXN-111

J.P. Lu[1], F.C. Christo[1] and D.L. Kennedy[2]

[1]Weapons Systems Division
Defence Science and Technology Organisation
P O Box 1500, Edinburgh, SA 5111 AUSTRALIA

[2]Orica Explosives, George Booth Drive
PO Box 196, Kurri Kurri, NSW

Abstract

An explicit finite element hydrocode, LS-DYNA, was used to model corner-turning shocks of a highly non-ideal PBXW-115 explosive. Unlike our previous work where the CPeX combustion model was used, this study has focused on the Ignition and Growth Reactive Model, which has been calibrated against experimental results. It was found that the Ignition and Growth Reactive Model performs as well as the CPeX model in predicting shock evolution around corners, yet both models were unable to accurately model the configuration of the brass confined explosive booster.

Introduction

PBXW-115 explosive has been tailored and fully qualified as an underwater explosive. Known also as PBXN-111 in the US, and PBXW-115(Aust), it is composed of 43% ammonium perchlorate (AP), 25% aluminium (Al), 20% RDX and 12% HTPB binder. Modelling this highly non-ideal explosive is a challenging task. Non-ideal explosives refer to explosives that have a C-J (detonation) pressure, velocity, or expansion isentrope significantly different from those expected from equilibrium, steady-state calculations. To this end, calculations of an axisymmetric geometry were performed using an explicit finite element hydrocode, LS-DYNA.

Earlier studies of PBXW-115 performance [6-9], have used the CPeX (Commercial Performance of explosives) reaction model to characterise this explosive in a cylindrical geometries. Kennedy and Jones [4] have also used the CPeX to model corner turning shocks to predict the breakout times through the curved surfaces of bowl-shaped acceptor charges. In this paper the capability of the Ignition and Growth Reactive Model (IGRM) to calculate corner turning shocks, is evaluated against the CPeX model and experimental data.

Model Description

The modelled geometry shown in Fig. 1, is based on the experiment of Forbes et al. [1,2]. The acceptor charges are spherically bowl-shaped PBXN-111 explosive. The curved surface of each bowl had a radius of curvature of 50.8 mm. The bowls were initiated through their flat rear surfaces by cylindrical boosters 50.8mm in diameter and 152.mm in length. Two different booster configurations were modelled here. The first was bare Comp-B (RDX/TNT explosive) booster and the second was PBXN-111 booster confined in a brass tube of 16.9mm wall thickness. In both cases the boosters were initiated by Pentolite charges.

Due to geometrical symmetry an axisymmetric computational model was constructed. The boosters were modelled with the programmed burn model and JWL equation of state. The acceptors were modelled with the Ignition and Growth Reactive Model, and the brass tube was modelled with the plastic-kinematic material model.

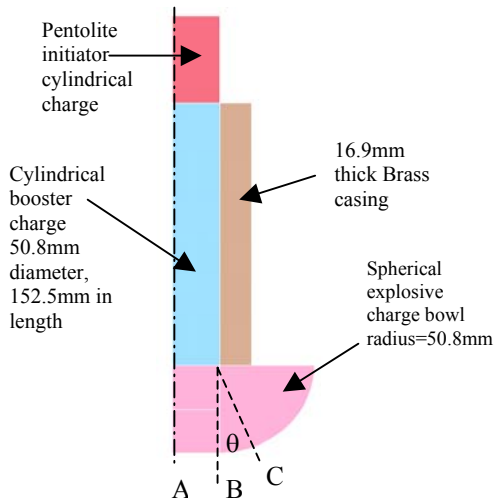

Figure 1. Schematic description of model geometry.

Both unreacted and combustion product equations of state are of Jones-Wilkins-Lee (JWL) form

$$P_{eos} = Ae^{-R_1 V} + Be^{-R_2 V} + \frac{\omega C_v T}{V} \quad (1)$$

where P_{eos} is pressure, V is relative volume, T is temperature, and A, B, R_1, R_2, ω (the Gruneisen coefficient) and C_v (the average heat capacity) are constants.

For the programmed burn model used for the boosters, the effect of combustion on the pressure in the high explosive regions is computed using

$$P = P_{eos} \max(F_1, F_2) \quad (2)$$

The burn mass fractions (F_1 and F_2) that control the release of chemical energy are computed by

$$F_1 = \begin{cases} \dfrac{2(t - t_1) DA_{e,\max}}{3\upsilon_e} & \text{if } t > t_1 \\ 0 & \text{if } t \le t_1 \end{cases} \quad (3)$$

$$F_2 = \frac{1 - V}{1 - V_{CJ}} \tag{4}$$

where t_1 is an ignition time that is computed for each computational element by dividing the distance from the detonation point to the centre of the element by the detonation velocity D. $A_{e,max,}$ and v_e are, respectively the maximum surface area and the volume of an element.

The JWL parameters and properties for Pentolite [10] that are used in the calculations are given in Table 1. Here ρ_0, and E_0 are the material density and initial internal energy, respectively.

Parameter	Pentolite
ρ_0 (g/cm^3)	1.65
A (GPa)	531.77
B (GPa)	8.933
R_1	4.6
R_2	1.05
ω	0.33
E_o (kJ/ cm^3)	8.0
D (mm/μs)	7.36

Table 1: Material and JWL parameters for Pentolite explosives.

Ignition and Growth Reactive Model

The Ignition and Growth Reactive Model is based on Tarver *et al.* [12] hypothesis that shock initiation of heterogeneous solid explosives should be modelled as at least a three-step process. The first step is the formation of hot spots created by various mechanisms (void closure, viscous heating, shear banding, etc.) during shock compression and the subsequent ignition (or failure to ignite due to heat conduction losses) of these heated regions. The second step in the process is assumed to be a relatively slow growth of reaction in inward and/or outward "burning" of the isolated hot spots. The third step in the shock initiation process is a rapid completion of the reaction as the reacting hot spots begin to coalesce. This model requires [11]:

- An unreacted explosive equation of state;
- A reaction product equation of state;
- A reaction rate law that governs the chemical conversion of explosive molecules to reaction product molecules; and
- A set of mixture equations to describe the states attained as the reactions proceed.

The chemical reaction rate equation in the three-term ignition and growth model is of the form [13]:

$$\frac{\partial F}{\partial t} = I(1-F)^b \left(\frac{\rho}{\rho_0} - 1 - a\right)^x + G_1 (1-F)^c F^d P^y + G_2 (1-F)^e F^f P^z \tag{5}$$

where F is the mass fraction of explosive (F=0 implies no reaction, F=1 implies complete reaction), t is time, ρ_0 is initial density, ρ is current density, P is pressure, and I, G_1, G_2, b, x, a, b, c, d, y, e, f, and z are constants. Upper threshold limits F_{mxig}, F_{mxGr} and F_{mnGr} are set to limit the contributions of the three terms to respectively; a maximum reacted fraction F_{mixg} for the first term, a maximum fraction F_{mxGr} for the second term and a minimum fraction F_{mnGr} for the last term. Accordingly, the ignition rate is set equal to zero when $F \geq F_{mixg,}$ the growth rate is set to zero when $F \geq F_{mxgr}$, and the completion rate is set to zero when $F \leq F_{mngr}$. These limits are material dependant.

Table 2 lists the calibrated parameters in the Ignition and Growth Reactive Model for unconfined PBXN-111 [8,9].

Unreacted Equation of State and Constitutive Values			
ρ_0(g/cm^3)	1.792	R_2	3.6
A(GPa)	4.06x10^3	$R_3 = \omega^* C_v$ (GPa/K)	2.09x10^{-3}
B(GPa)	-133.9	Yield Strength (GPa)	0.2
R_1	7.2	Shear Modulus (GPa)	4.54
Reacted Product Equation of State and CJ Values			
A (GPa)	372.9	$R_4 = \omega^* C_v$ (GPa/K)	4.884x10^{-4}
B (GPa)	5.412	E_o (KJ/cc)	12.95
R_1	4.453	D_{cj} (mm/μs)	6.476
R_2	1.102	P_{cj} (GPa)	20.84
Reaction Rate Parameters for 3 Term Model			
I (μsec^{-1})	30	G_2 (GPa^{-z}μsec^{-1})	1.805x10^{-03}
b	0.6667	e	1.0
a	0	f	0.1111
x	4.0	z	2.0
G_1 (GPa^{-y}μsec^{-1})	0.045	F_{mixg}	0.015
c	0.6667	F_{mxGr}	0.25
d	0.1111	F_{mnGr}	0
y	1.0		

Table 2. Parameters for the Ignition and Growth of Reaction Model [8,9]
Note: E_o is the internal energy.

These parameters are based on the assumption of the initial ignition and consumption of the RDX, the intermediate decomposition of the AP plus HTPB binder, and the later reaction of the aluminium.

For completeness of the presentation a brief description is also given on the CPeX model. Similar to the Ignition and Growth Reactive Model, the CPeX model represents the heat release rate as a three-term function in the form [4]

$$\frac{\partial F}{\partial t} = (1-F)\left(\frac{p_x a_h}{\tau_h} + \frac{p a_i}{\tau_i} + \frac{p a_f}{\tau_f}\right) \tag{6}$$

where F is the mass fraction of explosive, P is the pressure as computed from the JWL equation of state (Eq. 1). The three characteristics reaction times τ_h, τ_i, and τ_f are time constants of the hotspot, intermediate and final stages of the reaction, respectively. The a factors in Eq. 6, describe the assumed geometry of the burn front, controlling the switching on and off the hotspot, intermediate and final reaction rate terms. The detailed functional description of these factors, the function P_x and their calibrated values, are given in Ref.[4] and will not be repeated here.

Results

Time-dependant calculations were performed over a total time of 45 μsec. The time-step, which is adjusted automatically during the iterations, is selected to roughly correspond to the transient time of an acoustic wave through an element using the shortest characteristics distance in the computational domain. For numerical stability reasons, the size of time-step is scaled by a factor smaller than unity (0.9-0.67).

To compare the model with the experimental data [1,2], breakout time and pressure values are extracted from the model. Peak pressures at the outer surface of the bowl were presented as a function of a polar angle, θ (see Fig.1). The breakout time is defined as the time of arrival of a detonation wave at a given location on the outer surface of the bowl, relative to the time of arrival of the first detonation wave at the flat bottom of the bowl at location (A) in Fig. 1.

Figure 2 shows pressure contours of the detonation wave (for the PBXW/Brass booster) in the bowl approximately 31μs, 33μs, 36μs and 39μs after initiating the Pentolite charge.

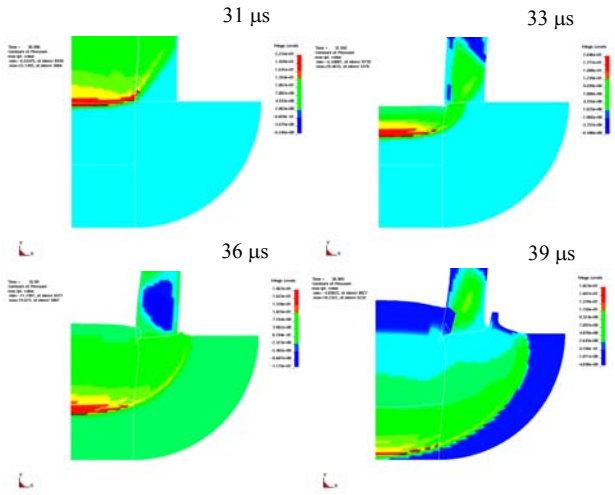

Figure 2: pressure (GPa) contours inside the bowl (for a PBXW/Brass booster configuration) 31μs, 33μs, 36μs and 39μs post initiation (note: pressure scales differ in each plot).

The figure shows the detonation front maintains almost a flat profile up to a 5μs after it enters the bowl, then it bends and begins to take the shape of the bowl. The model shows a slight increase in the peak shock pressure in the booster approximately 1μs after the shock entered the bowl, from ~21.5GPa to ~22.15GPa. The peak pressure then drops to 20.5GPa, 19.7GPa, and 18.2 GPa, respectively 2μs, 4μs, and 9μs after the shock enters the bowl.

It is interesting to note in Fig. 2, the time delay in the dynamic response of the brass tube. Tube deformation becomes obvious only a few microseconds after the detonation wave have entered the bowl. This is clearly illustrated in Fig. 2 at 31μs, which shows a flat detonation front entering the bowl at the explosive rear surface, while the oblique shock in the brass tube lags behind it. It is worth indicating the highly deformed computational elements of the brass tube were removed during iterations to reduce the possibility of numerical instability.

Burn mass fraction contours (F) for the PBXW/Brass booster configuration, inside the bowl are shown in Fig. 3. The figure shows a maximum of 62% and 65% mass burn fractions at 36μs and 39μs, respectively after the Pentolite initiation. This incomplete burnout of the explosives is consistent with typical burnout percentages of non-ideal explosives. Comparing the pressure (Fig. 2) and mass burn fraction (Fig. 3) contours, show a spatial lag of the reaction zone behind the detonation front.

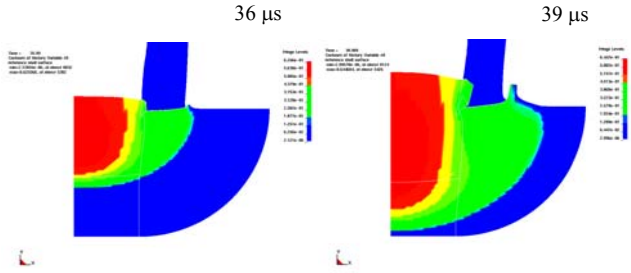

Fig. 3: Contours of mass burn fraction inside the bowl for a PBXW/Brass booster 36μs (left) and 39μs (right) post the Pentolite initiation.

Breakout times against angle (θ) are plotted in Fig. 4 for the COMP-B bowl charge and in Fig. 5 for the PBXW/Brass bowl charge. Results from the CPeX model [4] are also presented on the graphs.

For the COMP-B booster configuration, the results in Fig. 5 show that the Ignition and Growth Reactive Model predicts the breakout times reasonably accurate both in term of pressure magnitude and profile shape, consistent with the experiment. Both the IGRM and the CPeX models have comparable accuracy that is within the bounds of the experimental error, as shown in Fig.4.

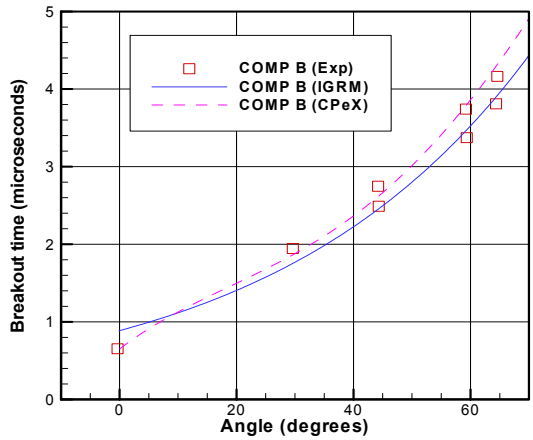

Fig. 4: A comparison between measured and calculated breakout times at various angular locations for a COMP-B booster, using the CPeX [4] and ignition and growth reactive model (IGRM).

However, for the PBXW/Brass booster configuration (Fig. 5), the IGRM performance is unexpectedly poor. The deviation of the calculated breakout times from the measured values increases with the angle, reaching a relative error of ~40% at an angle of 60 degrees. It is well known that having a brass casing (especially as thick as that used in this configuration) should increase the peak value and duration of the pressure delivered by the booster to the bowl charge, hence the breakout time through the outer edges of the bowl should be shortened. This was not the case here and no physical explanation can be found. Similar observations were made by Kennedy and Jones [4], who also could not find a physical explanation for this discrepancy.

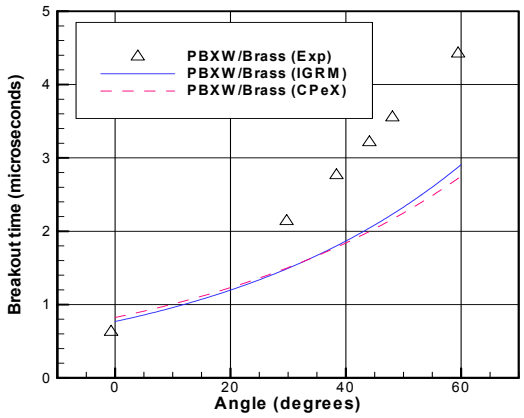

Fig. 5: A comparison between measured and calculated breakout times at various polar locations for PBXW/Brass booster, using the CPeX [4] and ignition and growth reactive model (IGRM).

It is worth mentioning that calculations were also performed using the IGRM (instead of the programme burn model) for the PBXN-111 booster, but did not yield any improvement in accuracy.

Considering the excellent agreement of the COMP-B booster configuration, the consistency and similarity of the results obtained by the IGRM and the CPeX models [4] for the PBXW/Brass booster configuration, implies that the current model parameters warrant further analyses for non-ideal explosives used in the complex geometries.

Conclusions

The modelling results using the Ignition and Growth Reactive Model for the COMP-B booster configuration are within the bounds of experimental error. However for the PBXW/Brass booster configuration the IGRM results were poor in comparison to the experiment. Similar conclusions were also obtained using the CPeX model. Considering that the IGRM parameters were calibrated using unconfined charges as it is the case in the bowl charges of this study and the good agreement for the COMP-B booster configuration, the only plausible explanation for the discrepancies point out to the suitability of otherwise of the programmed burn model, which was used for the boosters. This would the subject of our next investigation.

References

[1] Forbes, J.W., Lemar, E.R. and Baker R.N. (1989) *Detonation Wave Propagation in PBXW-115*, Proceedings of the 9th International Detonation Symposium, Office of the Chief of Naval Research, OCNR 113291-1, pp.806-815.

[2] Forbes, J.W., Lemar, E.R., Sutherland G.T. and Baker R.N. (1992) *Detonation Wave Curvature, Corner Turning and Unreacted Hugoniot of PBXN-111*, NSWCDD/TR-92/164.

[3] Jones, D.A., Kemister, G. and Borg, R.A.J. (1998) "Numerical simulation of detonation in condensed phase explosives", DSTO-TR-0705.

[4] Kennedy, D.L. and Jones, D.A. (1993) *Modelling Shock Initiation and Detonation in the Non Ideal Explosive PBXW-115*, Proceedings of the 10th International Detonation Symposium, Boston, Mass., USA, 12-16 July, Office of Naval Research ONR 33395-12, pp. 665-674.

[5] Lee, E.L. and Tarver C. M. (1980) *Phenomenological model of shock initiation in heterogeneous explosives*, Phys. Fluids, Vol. 23, pp.2362.

[6] Lu, J.P. (2001) *Evaluation of the Thermochemical Code – CHEETAH 2.0 for Modelling Explosives Performance,* DSTO-TR-1199, AR-011-997, DSTO Technical Report, Melbourne, August.

[7] Lu, J.P. and Kennedy, D.L. (2001) *Modelling of non-ideal explosive PBXW-115*, In PARARI 2001, Proceedings of 5th Australian Explosive Ordnance Symposium, 31 Oct. – 2 Nov., Canberra, Australia.

[8] Lu, J.P., Dorsett, H. and Kennedy, D.L. (2002) *Simulation of Aquarium Tests for PBXW-115(Aust)*, Proceedings of the 12th International Detonation Symposium, San Diego, California, USA, 11-16 August.

[9] Lu, J.P. and Kennedy, D.L. (2003) *Modelling of PBXW-115 Using Kinetic CHEETAH and the DYNA Codes*, DSTO-TR-1496, AR-012-899, DSTO Technical Report, Melbourne, September.

[10] Lu, J.P., Anderson, J.G. and Christo, F.C. (2004) *Detonation Modelling of High Explosive Cylinders,* Proceedings of the 24th International Symposium of Shock Waves, 11-16 July, Beijing, China.

[11] Murphy, M.J., Lee E.L., Weston, A.M. and Williams, A.E.(1993) *Modeling Shock Initiation in Composition B*, Proceedings of the 10th International Detonation Symposium, Boston, Mass., USA, 12-16 July, Office of Naval Research ONR 33395-12, pp.963-970.

[12] Tarver, C.M., Hallquist, J.O. and Erickson, L.M. (1985) *Modeling Short Pulse Duration Shock Initiation of Solid Explosives*, Proceedings of the 8th International Detonation Symposium, Naval Surface Weapons Center, Albuquerque, NSWC MP 86-194, pp.951-961.

[13] Tarver C.M. and Green L.G. (1989) *Using Small Scale Tests to Eestimate the Failure Ddiameter of a Propellant*, Proceedings of the 9th International Detonation Symposium, Office of the Chief of Naval Research, OCNR 113291-1, pp.701-710.